Global plasma simulation of charge state distribution inside a 2.45 GHz ECR plasma with experimental verification

2010 Plasma Sources Sci. Technol. 19 045024

(http://iopscience.iop.org/0963-0252/19/4/045024)

Plasma Sources Sci. Technol. **19** (2010) 045024 (6pp) doi:10.1088/0963-0252/19/4/045024

Global plasma simulation of charge state distribution inside a 2.45 GHz ECR plasma with experimental verification

M Bodendorfer[1], P Wurz and M Hohl[2]

Space Research and Planetary Sciences, University of Bern, 3012 Bern, Switzerland

E-mail: bodendorfer@ep.isas.jaxa.jp

Received 5 November 2009, in final form 21 June 2010
Published 23 July 2010
Online at stacks.iop.org/PSST/19/045024

Abstract

For the first time, the charge state distribution inside the MEsskammer für FlugzeitInStrumente und Time-Of-Flight (MEFISTO) electron cyclotron resonance (ECR) plasma and in the extracted ion beam was successfully simulated. A self-consistent ECR plasma ionization model (Hohl M 2002 MEFISTO II: Design, setup, characterization and operation of an improved calibration facility for solar plasma instrumentation *PhD Thesis* University of Bern) was further developed, recomputing the ion confinement time for every ion species and in every time step based on the actual plasma potential rather than using a prescribed constant ion confinement time. The simulation starts with a user defined set of initial conditions and develops the problem in time space by an adaptive step length fourth order Runge–Kutta (RK4) solver, considering particle densities based on ionization rates, recombination rates, ion confinement times and plasma potential. At the simulation end, a steady-state ion charge state distribution is reached, which is in excellent agreement with the measured ion beam charge state distribution of the MEFISTO ion source for Ar^{1+} to Ar^{5+} and in good agreement for Ar^{6+}.

(Some figures in this article are in colour only in the electronic version)

1. Introduction

The development of advanced permanent magnetic materials, able to supply magnetic fields for ECR frequencies of 10 GHz and more [4], makes the application of solenoids for plasma confinement in ECR ion sources obsolete in many new developed high voltage particle accelerators. The charge state distribution of an ion source critically depends on its design parameters, especially the magnetic confinement field and the excitation frequency. Consequently, the choice of a permanent magnetic confinement asks for a precise planning and design [3] before the production process due to very limited possibilities of field manipulation after the production of the magnetic confinement system. This paper presents a numerical simulation of the argon charge state distribution inside the MEFISTO ECR ion source and allows us to simulate future ECR sources before production, thereby significantly improving a successful ion source realization with the desired charge state distribution.

In this paper we present the plasma simulation in section 2 and its simulation results in section 3. In section 4 we discuss the simulation results, followed by our conclusion in section 5.

2. The plasma simulation

First, the existing plasma model by Hohl *et al* [5] is presented in section 2.1, followed by modifications to the model in section 2.2 and the numerical implementation in section 2.3.

2.1. The existing plasma model

The concept of a self-consistent ECR plasma model [5] was used to develop the presented numerical simulation. The plasma model aims at keeping the free parameters as low as possible to ensure simplicity and reliability compared with earlier, more sophisticated and more complex plasma models

[1] Present address: JAXA-ISAS, Kanagawa, Sagamihara, Japan.
[2] Present address: TOFWERK AG, 3600 Thun, Switzerland.

[2, 12–15]. The model concept is based on particle density balance (equation (1)):

$$\mathrm{d}N_j/\mathrm{d}t = \text{source-sink-loss} \tag{1}$$

with N_j denoting the respective particle density of charge state j, neutrals and electrons. The plasma model considers ionization and recombination rates, IR and RR, respectively, using two electron populations at two fixed temperatures, for the cold and the hot electron population [2]. The reaction rates [16, 17] are linearly combined using a fixed fraction of hot electrons $f_{\mathrm{h/e}}$ (equations (2) and (3)):

$$\mathrm{IR}_{j-1,j} = f_{\mathrm{h/e}} \cdot \mathrm{IR}^{\mathrm{hot}}_{j-1,j} + (1 - f_{\mathrm{h/e}}) \cdot \mathrm{IR}^{\mathrm{cold}}_{j-1,j}, \tag{2}$$

$$\mathrm{RR}_{j+1,j} = f_{\mathrm{h/e}} \cdot \mathrm{RR}^{\mathrm{hot}}_{j+1,j} + (1 - f_{\mathrm{h/e}}) \cdot \mathrm{RR}^{\mathrm{cold}}_{j+1,j}, \tag{3}$$

where $f_{\mathrm{h/e}}$ is the fraction of hot electrons present in the ECR plasma, $\mathrm{IR}^{\mathrm{hot}}_{j-1,j}$ is the ionization rate for the hot electrons, $\mathrm{IR}^{\mathrm{cold}}_{j-1,j}$ is the ionization rate for the cold electrons. $f_{\mathrm{h/e}}$ is a free parameter, i.e. it is not derived from the model but can be chosen by the user based on experimental evidence for the ECR ion source under investigation (in the range 1–30%).

Ionization is known to be a step-by-step process [2, 5] where double ionization from Ion^{j+} to $\mathrm{Ion}^{(j+2)+}$ can be neglected and single ionization from Ion^{j+} to $\mathrm{Ion}^{(j+1)+}$ is the dominant process. A neutral balance equation (equation (4)) and an ion balance equation array (equations (4)–(8)) are used to compute the time derivate for the fourth order Runge–Kutta (RK4) algorithm. The neutral gas density in the ion source is kept constant by the gas pressure regulation.

$$\frac{\mathrm{d}n_{\mathrm{gas}}(t)}{\mathrm{d}t} = 0, \tag{4}$$

$$\frac{\mathrm{d}n_1(t)}{\mathrm{d}t} = n_{\mathrm{e}}(t) \cdot [n_{\mathrm{gas}}(t) \cdot \mathrm{IR}_{0,1} + n_2(t) \cdot \mathrm{RR}_{2,1} \tag{5}$$

$$-n_1(t) \cdot \mathrm{IR}_{1,2} - n_1(t) \cdot \mathrm{RR}_{1,0}] - \frac{n_1(t)}{\tau_{\mathrm{ion},1}}, \tag{6}$$

$$\vdots$$

$$\vdots$$

$$\frac{\mathrm{d}n_j(t)}{\mathrm{d}t} = n_{\mathrm{e}}(t) \cdot [n_{j-1}(t) \cdot \mathrm{IR}_{j-1,j} + n_{j+1}(t) \cdot \mathrm{RR}_{j+1,j}$$

$$-n_j(t) \cdot \mathrm{IR}_{j,j+1} - n_j(t) \cdot \mathrm{RR}_{j,j-1}] - \frac{n_j(t)}{\tau_{\mathrm{ion},j}}, \tag{7}$$

$$\vdots$$

$$\frac{\mathrm{d}n_{\max}(t)}{\mathrm{d}t} = n_{\mathrm{e}}(t) \cdot \Big[n_{\max-1}(t) \cdot \mathrm{IR}_{\max-1,\max} - n_{\max}(t)$$

$$\cdot \mathrm{RR}_{\max,\max-1}\Big] - \frac{n_{\max}(t)}{\tau_{\mathrm{ion},\max}}, \tag{8}$$

$$\frac{\mathrm{d}n_{\mathrm{e}}(t)}{\mathrm{d}t} = n_{\mathrm{e}}(t) \cdot \Bigg[n_{\mathrm{gas}} \cdot \mathrm{IR}_{0,1} \sum_{j=1}^{\max-1} N_j(t) \cdot \mathrm{IR}_{j,j+1}$$

$$- \sum_{j=1}^{\max} N_j(t) \cdot \mathrm{RR}_{j,j-1}\Bigg] - \frac{n_{\mathrm{e}}(t)^{3/2}}{a \cdot t_{\mathrm{e}}}, \tag{9}$$

where n_{gas} is the neutral gas density, n_j is the ion density of charge state j, $\mathrm{IR}_{j-1,j}$ is the ionization rate from charge state $j-1$ to charge state j, $\mathrm{IR}_{j+1,j}$ is the recombination rate from charge state $j+1$ to charge state j and $t_{\mathrm{ion},j}$ is the mean ion confinement time. A similar balance equation is used [5] for the electron population (equation (9)).

2.2. *Modifications to the existing plasma model*

In the plasma model of Hohl *et al* 2002 [5], all particle confinement times $\tau_{\mathrm{ion},j}$ and τ_{e} are fixed. This allows a computationally economic implementation and it gives direct control over these parameters. However, due to fixed confinement times, the model is not able to simulate loss or keeping of particles depending on the actual plasma state and quasi-neutrality is not ensured, leading to a plasma potential which does not agree with theory or measurements. The modified plasma model makes use of combined magnetic and electrostatic confinement times for ions, updated in every computation step.

The magnetic confinement is provided by the permanent magnetic setup, which also provides the ECR field.

In addition, hot ECR electrons feature a strong anisotropic velocity distribution with preference perpendicular to the local magnetic field direction [1] resulting from the ECR heating process. This leads to a negligible loss cone fraction and a very good confinement before the respective hot electrons are lost due to scattering or ionization. Cold electrons are supposed to feature an isotropic velocity distribution equal to one of the ions. At the same kinetic energy and local magnetic field, electrons have a smaller Larmor radius than ions, which improves cold electron confinement compared with the ion confinement. All this leads to a slightly negative plasma potential [4, 10, 11], experimentally verified by Golovanivsky and Melin in 1992 [7]. The negative plasma potential ensures a proper confinement of the ions, long enough for step-by-step ionization up to high charge states.

The actually used ion confinement time is calculated by equation (10), according to Geller [2] and modified by a an additional parameter to allow linear modification of the ion confinement time (see section 4).

$$\tau_{\mathrm{ion},j} = r_{\mathrm{m}} \cdot L_{\mathrm{m}} \cdot a \cdot \sqrt{\frac{\pi\, m_{\mathrm{i}}}{2\, T_{\mathrm{i}}}} \cdot \exp\left(\frac{j \cdot \Phi}{T_{\mathrm{i}}}\right). \tag{10}$$

Here, r_{m} is the magnetic mirror ratio, L_{m} the mirror length given by its two maxima, m_{i} the ion mass, T_{i} the ion temperature, j the charge state of the respective ion species and Φ is the plasma potential. The bulk of the electrons is represented by cold electrons [2]. Their kinetic energy distribution and their scattering pattern with respect to the local magnetic field can be assumed to be isotropic. Since the geometric extent of the ECR plasmoid is much larger (plasma diameter: 26 mm) than the plasma Debye length (34 μm), we can assume quasi-neutrality and a homogeneous charge state distribution inside the approximately spherical ECR plasmoid. Then we can calculate the plasma potential by equation (11):

$$\Phi = \frac{\rho \cdot r_{\mathrm{pl}}^2}{6\, \epsilon_0} \tag{11}$$

Table 1. Summary of initial conditions and simulation parameters for the plots shown in figures 1 and 2.

	Value	S
Initial conditions		
Electron density	100 (cm^{-3})	u
Ion density	0 (cm^{-3})	u
Gas density	4.83×10^{10} (cm^{-3})	u
Mirror ratio	4.15	[5]
Argon ion mass	39.95 (amu)	
Confinement time τ_e	160 (s)	u
Hot electron fraction	0.25	u
Hot electron temp.	1700 (eV)	[6]
Cold electron temp.	1.7 (eV)	[5]
Ion temperature	1.7 (eV)	[5]
Simulation parameters		
maxerror	10^{-8}	u
Initial time step size	10^{-10} (s)	u
Ion conf. modifier a	2.0	u

Note: S—Source of parameter value, u—user defined.

with ρ as the total plasma charge density and r_{pl} the plasma radius.

By updating the plasma potential Φ and the ion confinement time $\tau_{ion,j}$ in every time step, this method effectively regulates charge imbalance in a realistic way. It directly affects the ion densities by lowering or increasing the respective ion confinement time based on the actual electron and ion densities. In contrast, the electron confinement time had to be fixed in order to enable a successful plasma density evolution, which is discussed below.

2.3. The numerical implementation

A fourth order Runge–Kutta method with adaptive step length was developed to solve the given set of equations (equations (5)–(9)). To optimize development time and computational performance Python was chosen as a programming language, using the Numpy extension for array handling.

The implemented adaptive step length algorithm uses a double step length result in every other iteration to compare with the result of the actual step length. The step length is decreased, if the relative difference between double and single step length result is larger than a user defined threshold maxerror, otherwise the step length is increased. A simulation run for Ar^{1+} to Ar^{8+} and maxerror $= 10^{-8}$ takes 5 h on an Intel Core 2 Duo 2.8 GHz system with 2 GB of RAM using only one of the two available CPU cores and a Xubuntu 8.10 operating system.

3. Simulation results

To obtain a best fit to the measured ion charge state distribution of the MEFISTO ion beam, the used initial conditions and simulation parameters are given in table 1.

The two parameters $f_{h/e}$ and the ion confinement time modifier a are connected and are based on experimental evidence. For a 2.45 GHz ECR ion source such as MEFISTO,

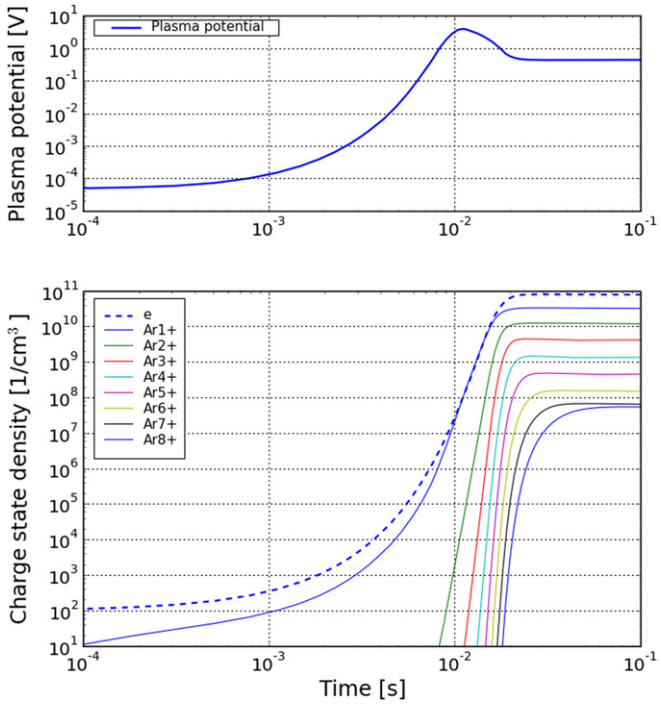

Figure 1. Simulated time evolution of the absolute value of the MEFISTO ECR plasma potential in the upper graph. The plasma potential remains negative throughout the whole simulation (see table 2 for the steady-state result). In the lower graph, the plasma electron density e and the ion charge state densities from Ar^{1+} to Ar^{8+} are plotted.

$f_{h/e}$ will not be above 0.5 due to the limited ionization states measured in the extracted ion beam. In order to keep $f_{h/e}$ below 0.5, the ion confinement time modifier $a = 2.0$ is chosen. This allows us to use a value $f_{h/e} = 0.25$. Figure 1 shows the simulation result of the plasma state time evolution for the electron density, all simulated ion charge state densities and the plasma potential.

The resulting time evolution of the plasma state is continuous for all simulation parameters. The electron density and the density of every charge state is monotonically increasing and reach steady state before 0.1 s in agreement with the experimental observations. The time evolution of the plasma potential features a maximum at 0.01 s and declines to −0.41 V which is in agreement with the literature values [4, 7]. In addition, we observe an exponential growth of the higher argon charge states around 0.01 s, the time of maximum plasma potential. Table 2 gives a summary of the simulated steady-state plasma particle density and the plasma potential values. Table 3 gives the electron confinement time applied as a simulation parameter and the ion confinement times resulting from the magnetic mirror, the updated plasma potential and the ion confinement time modifier $a = 2.0$ at steady state.

The simulation delivers *ad hoc* the charge state distribution inside the ECR plasma. However, to verify the simulated ion charge state densities with a measured ion charge state distribution of the extracted ion beam of MEFISTO, the simulation result needs to be modified by an extraction function. Due to the charge-state-sensitive combined magnetic and electrostatic confinement of the ions (see equation (10)),

Table 2. Summary of the fixed neutral density, the simulated steady-state particle densities, the plasma potential, the combined plasma charge density in elementary charges q cm^{-3} and the confinement parameter $n_e \cdot \tau_{i,4}$ (see section 4) of the MEFISTO ECR plasma.

Particle species	Simulation result
Neutrals (fixed)	4.83×10^{10} (cm^{-3})
Electrons	8.17×10^{10} (cm^{-3})
Ar^{1+}	3.44×10^{10} (cm^{-3})
Ar^{2+}	1.28×10^{10} (cm^{-3})
Ar^{3+}	4.39×10^{9} (cm^{-3})
Ar^{4+}	1.34×10^{9} (cm^{-3})
Ar^{5+}	4.05×10^{8} (cm^{-3})
Ar^{6+}	1.18×10^{8} (cm^{-3})
Ar^{7+}	4.41×10^{7} (cm^{-3})
Ar^{8+}	2.81×10^{7} (cm^{-3})
Plasma potential	-0.41 (V)
Charge density	-8.1×10^{5} (q cm^{-3})
$n_e \cdot \tau_{ion,4+}$	1.73×10^{8} (s cm^{-3})

Table 3. Used electron and computed ion confinement times in the steady state of the MEFISTO simulation.

Particle species	Confinement time (s)
electrons (fixed)	160.0
Ar^{1+}	4.05×10^{-4}
Ar^{2+}	6.12×10^{-4}
Ar^{3+}	9.24×10^{-4}
Ar^{4+}	1.40×10^{-3}
Ar^{5+}	2.11×10^{-3}
Ar^{6+}	3.19×10^{-3}
Ar^{7+}	4.81×10^{-3}
Ar^{8+}	7.27×10^{-3}

the extracted ion beam has a different charge state distribution than the plasma itself. Generally, low ion charge states can be extracted more successfully than higher ion charge states due to the different charge-to-mass ratio. Equation (12) [2] transforms the plasma ion charge state distribution into the extracted charge state distribution:

$$I_j \sim n_j \cdot \sqrt{\frac{e \cdot T_e}{m_i}} \cdot r_{pl}^2 \cdot \frac{1}{r_m} \cdot \exp\left(\frac{j \cdot \Phi}{T_i}\right) \qquad (12)$$

with I_j the ion beam current of charge state j, n_j the ECR plasma ion density for charge state j, e the electron elementary charge, T_e the cold electron temperature in eV, m_i the ion mass in kg, r_{pl} the plasma radius in m, r_m the magnetic mirror ratio and T_i the ion temperature in eV. Figure 2 shows the comparison between the simulated ion charge state distribution in the ECR plasma, the corrected extracted simulation ion beam and the measured extracted ion beam from MEFISTO. All densities and currents are normalized to Ar^{1+}.

We can see the simulated argon charge state distribution in the ion source to be significantly higher than the simulated extracted ion distribution, which is expected from equation (12). In addition, the argon charge state distribution of the simulated and corrected extracted ion beam is in excellent agreement with the measured charge state distribution of the extracted MEFISTO ion beam for Ar^{1+} to Ar^{5+}. The simulated

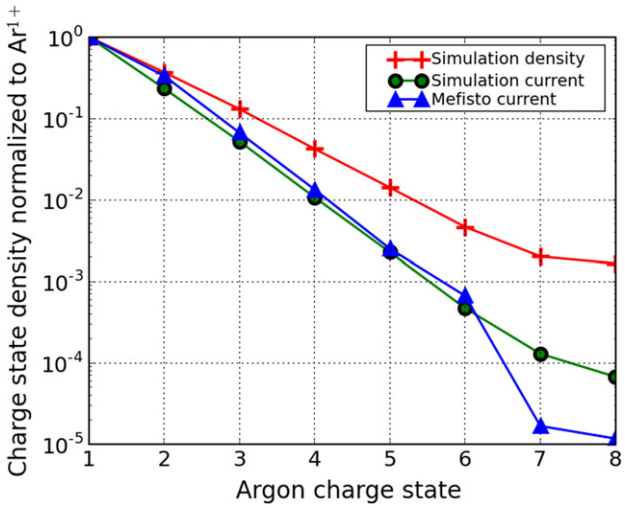

Figure 2. Comparison of the simulated charge state distribution inside its ECR plasma, the corrected distribution for the extracted ion beam and the measured charge state distribution in the extracted ion beam of MEFISTO [5].

charge state of Ar^{6+} is slightly lower than the measured one. And the measured charge states of Ar^{7+} and Ar^{8+} are significantly lower than the simulated ones.

4. Discussion

The shortfall of the measured Ar^{7+} and Ar^{8+} ion currents in MEFISTO compared with the simulation result may be explained as follows. The simulation uses a simple and robust macroscopic plasma model including plasma potential time evolution. More complex or microscopic plasma phenomena are not considered such as geometry dependent oscillations, wave phenomena or higher order ionization mechanisms. Hence the expected, simple exponential regress of the simulated charge state distribution. In addition, the background particle density (i.e. the residual gas) in the beam transport system of MEFISTO causes charge exchange between the neutral gas molecules and the multiply charged ions, reducing their charge by one at each charge exchange event. The probability for this charge exchange rises non-linearly with the charge states and results in a preferential loss of higher charge states. This agrees with the slight surplus of Ar^{6+} in the measurement compared with the simulation. Furthermore, the parameters of the ion optics, facilitating the beam transport from the ion source to the ion current collector, can be optimized for a single charge state only. This penalizes other charge states.

In the literature [2], equation (10) without the additional ion confinement time modifier a is based on the assumption that an ion is experiencing about one bounce in the magnetic mirror on average before being lost through the mirror loss cone by scattering. To obtain a simulation result in good agreement with the measurement and to keep the hot electron fraction $f_{h/e}$ as low as 0.25, an ion confinement time modifier $a = 2.0$ had to be chosen. Therefore, the parameter a can be interpreted as an ion experiencing two bounces on average in the magnetic mirror before being lost through the loss cone instead of being

lost after only one bounce. Due to the approximative nature of the one-bounce theory, this slight modification is considered to be acceptable.

The resulting electron density does not exceed the cut-off density given by the MEFISTO microwave frequency. The electron density of the simulation result is therefore in excellent agreement with the literature [1, 2]. However, to obtain the presented electron density in the simulation in order to provide the necessary ionization basis and the plasma potential, an average electron confinement time of 160 s is required. The presented plasma model does not take into account secondary electrons emitted from the plasma chamber wall, nor does it distinguish between a cold and a hot electron population in the time evolution. In a modified simulation, in which the contribution of secondary electrons from walls to the plasma is considered, the electron confinement time of 160 s can be reduced by at least a factor of 10 to maintain the otherwise same simulation parameters and to obtain identical simulation results. The importance of secondary electrons for the ECR plasma has been recognized in several experiments [18–21].

To produce multi-charged ions with low atomic Z number, Geller [2] requires $n_e/n_0 > 1$, $n_e \cdot \tau_i \sim 10^8$ ($s\,cm^{-3}$) and $T_{ecold} < 100$ eV. For argon and a medium charge state of Ar^{4+}, all these requirements are fulfilled by the results of our simulation.

A previous global ECR plasma model by Oda *et al* [8] use constant ion confinement times which are independent of the respective ion charge states. In our simulation, the ion confinement time is recomputed in every time step based on the actual plasma potential which, in turn, is also recomputed in every time step based on the actual electron density and the charge state distribution. In addition, Oda *et al* uses a different set of ion balance equations with additional sum terms, also considering direct ionization from neutrals to higher charge states as opposed to our model which uses single step ionization only (see section 2.1).

Another previous global ECR plasma model by Skalyga *et al* 2006 [9] simulates an opposing solenoid, pulsed and high power ECR plasma of a different kind. The resulting electron densities are three orders of magnitude higher than in our experiment and our simulation. In addition, Skalyga *et al* use a 37.5 GHz microwave pulse width of no more than 1.5 ms. In contrast, the MEFISTO plasma simulation suggests that its 2.45 GHz ECR plasma becomes stationary only after 100 ms. As a consequence, this simulation and this experiment are both highly significant in their own right, our simulation is not in contradiction with, nor is it contradicted by those other findings.

5. Conclusion

The presented simulation is able to deliver a charge distribution which is in excellent agreement with the measured charge state distribution of MEFISTO from Ar^{1+} to Ar^{5+} and in good agreement for Ar^{6+}. The difference for Ar^{7+} and Ar^{8+} can be explained by charge exchange phenomena and ion optics transfer loss.

Furthermore, in this simulation a double bounce input parameter in the magnetic mirror of MEFISTO is necessary to confine the ions long enough to result in the measured charge state distribution and in order to limit the hot electron fraction as low as 0.25.

Acknowledgment

The authors gratefully acknowledge the financial support by the Swiss National Science Foundation.

References

[1] Chen F F 1984 *Introduction to Plasma Physics and Controlled Fusion Vol 1: Plasma Physics* 2nd Edn (New York: Plenum)
[2] Geller R 1996 *Electron Cyclotron Ion Sources and ECR Plasmas* (Bristol: Institute of Physics Publishing)
[3] Bodendorfer M, Altwegg K, Shea H and Wurz P 2008 Identification of the ECR zone in the SWISSCASE ECR ion source *Nucl. Instrum. Methods Phys. Res.* B **266** 4788–93
[4] Bodendorfer M 2008 SWISSCASE *PhD Thesis* Ecole Politechnique de Lausanne, Switzerland
[5] Hohl M 2002 MEFISTO II: Design, setup, characterization and operation of an improved calibration facility for solar plasma instrumentation *PhD Thesis* University of Bern
[6] Hohl M, Wurz P and Bochsler P 2005 Investigation of the density and temperature of electrons in a compact 2.45 GHz electron cyclotron resonance ion source plasma by x-ray measurements *Plasma Sources Sci. Technol.* **14** 692–9
[7] Golovanivsky K S and Melin G 1992 A study of the parallel energy distribution of lost electrons from the central plasma of an electron cyclotron resonance ion source *Rev. Sci. Instrum.* **63** 2886–8
[8] Oda K, Abe N, Yamamoto T and Kawanishi M 1981 Japanese Production mechanism in an ECR-type multiply-charged ion source *J. Appl. Phys.* **20** 955–61
[9] Skalyga V, Zorin V, Izotov I, Razin S, Sidorov A and Bohanov A 2006 Gasdynamic ECR source of multicharged ions based on a cusp magnetic trap *Plasma Sources Sci. Technol.* **15** 727–34
[10] Shirkov G D 1993 A classical model of ion confinement and losses in ECR ion sources *Plasma Sources Sci. Technol.* **2** 250
[11] Shirkov G D 1994 *Electron and ion confinement conditions in the open magnetic trap of ECR ion sources, CERN-PS-94-13*
[12] Melin G, Drentje A G, Girard A and Hitz D 1999 Ion behavior and gas mixing in electron cyclotron resonance plasmas as sources of highly charged ions *J. Appl. Phys.* **86** 4772–779
[13] Petty C C, Goodman D L, Smatlak D L and Smith D K 1990 Confinement of multiply charged ions in an cyclotron resonance heated mirror plasma *Phys. Fluids* B **3** 705–14
[14] Pras R and Lamoureux M 1998 Electron cyclotron resonance ion source ionic currents (both in the stable and periodic regimes) modeled in relation with the hot electron temperature via the potential dip *Rev. Sci. Instrum.* **69** 700–2
[15] Whaley D R and Gerry W D 1990 Ion temperature effects on ion charge-state distributions of an electron cyclotron resonant ion source *Phys. Fluids* B **2** 1195–203

[16] Arnaud M and Rothenflug R 1985 An updated evaluation of recombination and ionization rates *Astron. Astrophys. Suppl. Ser.* **60** 425–57
[17] Arnaud M and Raymond J 1992 Iron ionization and recombination rates and ionization equilibrium *Astrophys. J.* **398** 394–406
[18] Matsumoto K 1994 Role of a biased electrode in the first stage of electron cyclotron resonance multicharge ion source *Rev. Sci. Instrum.* **65** 1116
[19] Sekiguchi M 1996 Summary of 12th International ECRIS Workshop *Rev. Sci. Instrum.* **67** 1606
[20] Leitner M *et al* 1994 Single-stage 5 GHz ECR-multicharged ion source with high magnetic mirror ratio and biased disk *Rev. Sci. Instrum.* **65** 1091
[21] Melin G *et al* 1994 Status of development of ECR ion sources at Grenoble *Rev. Sci. Instrum.* **65** 1051